Magnetic Structures of Chromium-Modified Mn_2Sb

A. E. AUSTIN AND E. ADELSON
Battelle Memorial Institute, Columbus, Ohio

AND

W. H. CLOUD
Central Research Department, E. I. du Pont de Nemours and Company, Wilmington, Delaware

(Received 8 April 1963)

The magnetic structures of tetragonal chromium-modified Mn_2Sb have been determined by neutron-diffraction studies of single crystals. Compositions of $Mn_{2-x}Cr_xSb$ for x from 0.023 to 0.10 were examined. Three magnetic structures have been observed, depending upon composition and temperature. These all have antiferromagnetic coupling between manganese atoms Mn(I) in (a) sites of (0,0,0), $(\frac{1}{2},\frac{1}{2},0)$, and Mn(II) in (c) sites of $(0,\frac{1}{2},z)$, $(\frac{1}{2},0,\bar{z})$. The high-temperature structure is that of ferrimagnetic Mn_2Sb where there is ferromagnetic coupling between successive layers of Mn(I) plus adjacent Mn(II) atoms. With decreasing temperature there is an exchange inversion to an antiferromagnetic coupling between successive layers giving a magnetic unit cell with a tetragonal axis twice that of the x-ray cell. For $x=0.03$ a new weakly ferrimagnetic state exists between the ferrimagnetic and antiferromagnetic states. The magnetic unit cell of this structure has a tetragonal axis three times that of the x-ray cell. The spins are perpendicular to the c axis in this intermediate ferrimagnetic structure and in the antiferromagnetic state of the compositions studied.

INTRODUCTION

CHROMIUM-MODIFIED Mn_2Sb exhibits a transformation with decreasing temperature from a ferrimagnetic to an antiferromagnetic state.[1–3] The magnetic states with their temperature and composition ranges are described elsewhere.[4] This exchange inversion is a first-order transformation and the temperature at which it occurs T_s increases with increasing chromium content. Ferrimagnetic[5] Mn_2Sb has an anisotropy change at $T_A \approx 240°K$ with the magnetic moments arranged parallel to the c axis at higher temperatures and perpendicular at lower temperatures. The anisotropy temperature T_A decreases with increasing chromium content. Therefore, depending upon chromium content, T_s may be either above or below T_A. An intermediate state between the ferrimagnetic and antiferromagnetic states has been found for compositions $Mn_{2-x}Cr_xSb$ with $x<0.035$.[6] This intermediate state is weakly ferrimagnetic and the transitions from it to the higher temperature ferrimagnetic and the lower temperature antiferromagnetic states are first order. The initial paper[6] reported that the intermediate state was a spiral spin configuration. The structure of this state has been studied in detail by neutron diffraction. It was found that the structure is not strictly a spiral configuration.

This paper reports on neutron diffraction studies of the magnetic states of $Mn_{2-x}Cr_xSb$ for $x=0.10$, 0.05, 0.03, and 0.023.

CRYSTALLOGRAPHY

The structure of the chromium-modified compositions is that of Mn_2Sb, namely, tetragonal, $P4/nmm$. The manganese atoms in (a) positions, (0,0,0), $(\frac{1}{2},\frac{1}{2},0)$, are denoted as Mn (I), while those in (c) positions, $(0,\frac{1}{2},z)$, $(\frac{1}{2},0,\bar{z})$, are denoted as Mn (II) and the antimony atoms are also in (c) positions. The parameters $z_{Mn}=0.295$ and $z_{Sb}=-0.280$ have been determined.[5,7] The neutron intensities of nuclear (00l) reflections for 7 orders for the composition $x=0.10$ agreed with these parameters. Temperature factors were calculated for the Debye temperature of 300°K of Heaton and Gingrich.[7] The relative neutron intensities of (hh0) reflections at room temperature indicated a Debye temperature of about 280°K, in reasonable agreement with the x-ray data.

EXPERIMENTAL TECHNIQUES

The neutron-diffraction data were obtained from single crystals in the form of plates 0.5 cm×0.15 cm or of a cylinder 0.7-cm diam. The experiments were carried out on neutron spectrometers at the Battelle Research Reactor. A lead monochromating crystal gave an effective neutron wavelength of 1.12 Å. The crystals were heated or cooled by a gas stream or by mounting in a liquid-nitrogen cryostat with a temperature-controlled heater. An iron-constantan thermocouple at the base of the crystal was used for temperature measurements.

The crystals were rather imperfect, with a mosaic spread estimated to be about 30 min, according to back-reflection Laue x-ray patterns. For the largest crystal, estimates of the minimum mosaic spread to satisfy the

[1] T. J. Swoboda, W. H. Cloud, T. A. Bither, M. S. Sadler, and H. S. Jarrett, Phys. Rev. Letters **4**, 509 (1960).
[2] W. H. Cloud, H. S. Jarrett, A. E. Austin, and E. Adelson, Phys. Rev. **120**, 969 (1960).
[3] W. H. Cloud, T. A. Bither, and T. J. Swoboda, Suppl. J. Appl. Phys. **32**, 55 (1961).
[4] F. J. Darnell, W. H. Cloud, and H. S. Jarrett, Phys. Rev. **130**, 647 (1963).
[5] M. K. Wilkinson, N. S. Gingrich, and C. G. Shull, J. Phys. Chem. Solids **2**, 289 (1957).
[6] P. E. Bierstedt, F. J. Darnell, W. H. Cloud, R. B. Flippen, and H. S. Jarrett Phys. Rev. Letters **8**, 15 (1962).
[7] L. Heaton and N. S. Gingrich, Acta Cryst. **8**, 207 (1955).

thin-crystal criterion of Bacon[8] were 2 to 6 min. Comparison of strong and weak nuclear reflections with calculated structure factors showed a linear relationship; therefore, the effects of secondary extinction for these crystals were assumed negligible.

The neutron diffraction intensities of magnetic reflections for the ferrimagnetic states were obtained by subtraction of the nuclear contribution. The nuclear intensities were obtained by measurements either above the Curie temperature, or in the antiferromagnetic state. The nuclear contributions of the (00l) reflections were also measured at temperatures above T_A where the magnetic moments are parallel to the c axis and there is no magnetic contribution. The intensities were corrected for geometrical and temperature factors. The ratio of the nuclear intensities to the calculated structure factors $|F_n|^2$ was used to convert the magnetic intensities to magnetic structure factors. The magnetic form factors used were the same as those given for Mn_2Sb.[5] Recent studies[9] of Mn_2Sb using polarized neutrons show small differences between the form factors of Mn(I) and Mn(II), but give essential agreement with the results of Ref. 5. The nuclear structure factors were calculated on the basis of chromium substitution at random in the Mn(I) sites, as discussed in Appendix A.

The compositions $Mn_{1.9}Cr_{0.1}$ and $Mn_{1.95}Cr_{0.05}Sb$ had exchange inversion temperatures of 40 and -100°C, respectively. The composition $Mn_{1.97}Cr_{0.03}Sb$ had transition temperatures of -140°C from the high temperature ferrimagnetic to the intermediate weakly ferrimagnetic state and -160°C to the antiferromagnetic state. This composition also showed a definite ferrimagnetic anisotropy change at -55 to -60°C. The composition $Mn_{1.977}Cr_{0.023}Sb$ remained in the intermediate weakly ferrimagnetic state below its transition temperature of -190°C.

MAGNETIC STRUCTURE ANALYSIS

The neutron-diffraction patterns of these crystals have revealed three different magnetic structures. First there is the normal ferrimagnetic structure the same as that of Mn_2Sb,[5] where the magnetic unit cell is identical with the chemical one. The magnetic moments switch with decreasing temperature from parallel to perpendicular orientation with respect to the tetragonal axis. In the parallel orientation there is no magnetic-scattering contribution to the (00l) reflections.

The antiferromagnetic structure has a magnetic unit cell doubled along the c axis, as indicated by the additional (00l) and (hhl) reflections. The normal (00l) and (hhl) reflections were solely nuclear. As reported previously,[2,3] the antiferromagnetic coupling between adjacent Mn (I) and Mn (II) atoms is maintained as in the ferrimagnetic state. There is antiferromagnetic coupling between successive ferrimagnetic layers of Mn (I) plus adjacent Mn (II) atoms. The magnetic moments were found to be perpendicular to the c axis.

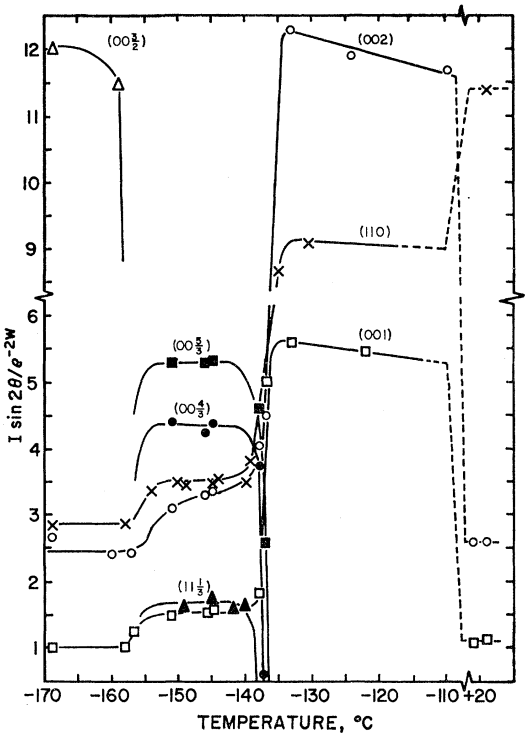

FIG. 1. Temperature dependence of ferrimagnetic reflections through the intermediate state of $Mn_{1.97}Cr_{0.03}Sb$.

The composition $x=0.03$ exhibits a third structure intermediate between the low-temperature Mn_2Sb ferrimagnetic state and the antiferromagnetic state existing at still lower temperatures. This is a weakly ferrimagnetic structure.[4,6] The (00l) and (hhl) reflections indicate a tripling of the periodicity along the c axis. There are magnetic contributions to both the (00l) and (hhl) nuclear reflections, with the relative ratios remaining as in the low-temperature Mn_2Sb ferrimagnetic state. This indicates that the magnetic moments remain perpendicular to the c axis.

All three magnetic states were studied in a crystal with composition $Mn_{1.97}Cr_{0.03}Sb$. Figure 1 shows the changes of intensity of reflections which indicate these transitions. All reflections are indexed in terms of the chemical unit cell. The magnetic-moment reorientation in the ferrimagnetic state occurs between -55 and -60°C, as shown by the increase of (002) and decrease of (110) reflections. The transition from the Mn_2Sb ferrimagnetic state to the intermediate state takes place at -138°C during cooling. Here the new reflections for the triple cell appear and the intensities of the normal reflections decrease. This intermediate ferrimagnetic state exists down to about -155°C. Below -159°C the triple-index reflections disappear, those of

[8] G. E. Bacon, *Neutron Diffraction* (Oxford University Press, New York, 1955).

[9] H. A. Alperin, J. P. Brown, and R. Nathans, Suppl. J. Appl. Phys. 34, 1201 (1963).

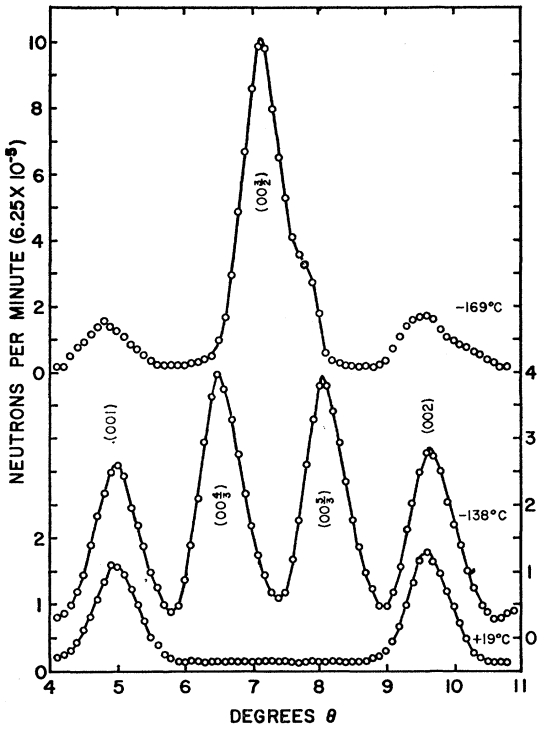

FIG. 2. (00l) reflections from $Mn_{1.97}Cr_{0.03}Sb$ at 19, −138, and −169°C for the ferrimagnetic, intermediate, and antiferromagnetic states, respectively. Scale values $\times 16 \times 10^3$ gives measured neutrons per minute.

the antiferromagnetic state with doubled cell appear, and the intensities of the normal ones, (110) and (002), decrease to their nuclear values. Figure 2 shows the (00l) reflection changes indicative of the ferrimagnetic, intermediate, and antiferromagnetic states. The (001) and (002) reflections at 19°C are solely nuclear. In the intermediate state at −138°C there is still a magnetic contribution to the intensities of the (001) and (002) reflections which disappears in the antiferromagnetic state at −169°C. Table I lists values of magnetic-reflection contributions $|F_0|^2q^2$ for this crystal in the three states. The values were calculated from the observed intensities relative to the nuclear intensities and were corrected for form, temperature, and geometrical factors. The values for the intermediate state at −145°C are averages of repeated measurements in the temperature range of −140 to −150°C over which the intensities remained essentially constant. The (1 1 $\frac{1}{3}$) and (1 1 $-\frac{1}{3}$) reflections were observed to be equal and, therefore, they were averaged together.

TABLE I. Observed magnetic contributions $|F_0|^2q^2$ of $Mn_{1.97}Cr_{0.03}Sb$.

Index	Nuclear[a] F_0^2	Ferri-magnetic, −135°C	Magnetic $\|F_0\|^2q^2$ intermediate state, −145°C	Antiferro-magnetic, −169°C
(0 0 2/3)	···	0	0	0
(0 0 1)	0.475	2.381	0.229	0
(0 0 4/3)	···	0	2.49	0
(0 0 3/2)	···	0	0	7.371
(0 0 5/3)	···	0	3.46	0
(0 0 2)	1.141	7.458	0.582	0
(0 0 7/3)	···	0	1.00	0
(0 0 5/2)	···	0	0	1.124
(0 0 8/3)	···	0	0	0
(1 1 0)	1.07	4.670	0.456	0
(1 1 1/3)	···	0	1.30[b]	0
(1 1 1/2)	···	0	0	2.307
(1 1 2/3)	···	0	0.510	0

[a] Calculated values.
[b] Average of both (1 1 $\frac{1}{3}$) and (1 1 $-\frac{1}{3}$).

The crystal with $x=0.023$ was examined at room temperature and in liquid nitrogen, −196°C. At room temperature, it has the Mn_2Sb ferrimagnetic structure. At −196°C, its magnetic structure is essentially the same as that observed for the intermediate state of $Mn_{1.97}Cr_{0.03}Sb$. Intensity measurements were not as accurate as for the $x=0.03$ crystal because of the background scattering of the liquid nitrogen.

STRUCTURE CALCULATIONS OF THE INTERMEDIATE STATE

The intermediate state in $Mn_{1.97}Cr_{0.03}Sb$ has a magnetization per gram slightly less than one-third that of the normal ferrimagnetic structure.[6] The magnetic contribution to the neutron diffraction intensities of the regular reflections is about 9% of that of the normal ferrimagnetic state, Table I. This also indicates a net moment of slightly less than one-third that of the Mn_2Sb ferrimagnetic state. The agreement of both types of data eliminates the possibility of a mixture of ferrimagnetic and antiferromagnetic phases.

The antiparallel alignment of adjacent Mn (I) and Mn (II) moments in ferrimagnetic layers is maintained in both the ferrimagnetic and antiferromagnetic states.[2,3] It, therefore, seems reasonable to assume that the Mn (I) and Mn (II) moments within a layer are also antiparallel in the intermediate state, and the discussion that follows is based upon this assumption. Furthermore, it is shown in Appendix B that if the angle between Mn (I) and Mn (II) moments is assumed to differ from π within a layer, the calculated relative intensities of the (00l) satellite reflections ($l=N\pm\frac{1}{3}$) do not agree with observed values.

The neutron diffraction pattern of the intermediate state contains a ferromagnetic component of $k=2\pi/c$ and an antiferromagnetic component of $k=2\pi/3c$. A helical structure of the type discussed by Koehler[10] appeared to be a possible structure. In the present case the structure would be a spiral arrangement of the ferrimagnetic layers with a common angle β between the moments and helix axis. The data of Table I for the intermediate state do not fit this type of structure. For example, calculated intensities for a simple antiferromagnetic helix $\beta=90°$, with axis parallel or perpendicular to c, are shown in Table II. Average values of the moments from the ferrimagnetic and antiferromagnetic

[10] W. C. Koehler, Acta Cryst. 14, 535 (1961).

TABLE II. Calculation of $|F_0|^2q^2$ of the intermediate state.

Index	$\|F_0\|^2q^2$ Observed (−145°C)	$\|F_0\|^2q^2$ Calculated Helix with axis ∥ to c	⊥ to c	Triple ferrimagnetic cell[a] $\beta=0°$	$\beta=18°$
(0 0 1/3)	···	0.232	0.116	0.206	0.186
(0 0 2/3)	0	0.042	0.021	0.038	0.034
(0 0 1)	0.229	0	0	0.247	0.222
(0 0 4/3)	2.49	3.12	1.56	2.78	2.50
(0 0 5/3)	3.46	4.26	2.13	3.80	3.42
(0 0 2)	0.582	0	0	0.756	0.680
(0 0 7/3)	1.00	1.45	0.725	1.29	1.16
(0 0 8/3)	0	0.123	0.061	0.11	0.10
(1 1 0)	0.450	0	0	0.475	0.428
(1 1 1/3)	1.30	1.68	2.46	1.49	1.34
(1 1 2/3)	0.510	0.666	0.92	0.60	0.540

[a] For $\Phi_i=\pi$ or $\Phi_j=\pi/2$.

states were used in the calculation. The calculated intensities of the $(l=N\pm\frac{1}{3})$ reflections for the helix with axis parallel to c are greater than the observed values but agree relatively. A decrease in the inclination angle β would decrease the satellite intensities but would yield only a magnetic contribution to the $(hh0)$ reflections and none to the $(00l)$ reflection. The relative intensities of the $(l=N)$ reflections are the same as those observed for the ferrimagnetic state (see Table I). Thus, the axis of the $2\pi/3c$ component is parallel to c, but the ferromagnetic component $2\pi/c$ is perpendicular to c. The net moments of each layer must, therefore, lie in the basal plane perpendicular to c.

The magnetization of a layer can be represented by vectors of constant magnitude having phase angles Φ_n in the basal plane, where $n=0, 1, 2$. Without loss of generality Φ_0 can be chosen to be zero. Since the neutron diffraction contains $k=2\pi/c$ and $k=2\pi/3c$ components, the magnetization of a layer can also be expressed as[11]

$$\mathbf{M}(n)=\mathbf{D}+\mathbf{U}\cos(2\pi n/3)+\mathbf{V}\sin(2\pi n/3), \quad (1)$$

where $\mathbf{U}$ and $\mathbf{V}$ are perpendicular and n takes the values 0, 1, 2. In order to make $|M(n)|$ the same for each layer, $\mathbf{D}\cdot\mathbf{V}=0$ and $4\mathbf{D}\cdot\mathbf{U}=V^2-U^2$. It follows that $\mathbf{M}(0)\cdot\mathbf{M}(1)=\mathbf{M}(0)\cdot\mathbf{M}(2)$. Thus, either $\Phi_1=\Phi_2$ or $\Phi_1=-\Phi_2$. Denoting these two cases by $\Phi_i=\Phi_1=\Phi_2$ and $\Phi_j=\Phi_1=-\Phi_2$ the intensities of the $(00l)$ and $(11l)$ reflections will be

$$\begin{aligned}
&|F_0|^2q^2(00l)\\
&=4/9(P_{\rm I}-P_{\rm II}\cos2\pi lz)^2\\
&\quad\times[(1+2\cos\Phi_i\cos2\pi l)^2+(2\sin\Phi_i\cos2\pi l)^2]\\
&=4/9(P_{\rm I}-P_{\rm II}\cos2\pi lz)^2\\
&\quad\times[(1+2\cos\Phi_j\cos2\pi l)^2+(2\sin\Phi_j\sin2\pi l)^2], \quad (2)\\
&|F_0|^2q^2(11l)\\
&=2/9(1+\cos^2\Theta)(P_{\rm I}+P_{\rm II}\cos2\pi lz)^2\\
&\quad\times[(1+2\cos\Phi_i\cos2\pi l)^2+(2\sin\Phi_i\cos2\pi l)^2]\\
&=2/9(1+\cos^2\Theta)(P_{\rm I}+P_{\rm II}\cos2\pi lz)^2\\
&\quad\times[(1+2\cos\Phi_j\cos2\pi l)^2+(2\sin\Phi_j\sin2\pi l)^2],
\end{aligned}$$

[11] D. H. Lyons, T. A. Kaplan, K. Dwight, and N. Menyuk, Phys. Rev. **126**, 540 (1962).

where l is the index based on the x-ray unit cell, Θ is the angle between the scattering vector and the c axis, $P_{\rm I}$ and $P_{\rm II}$ are the magnetic scattering lengths of Mn (I) and Mn (II) sites, respectively, and z is the position parameter of Mn (II) in the x-ray unit cell. For the case $\Phi_j=2\pi/3$ the structure is a simple helix with axis parallel to c, and the equations become identical with those of Koehler.[10]

Using an average of the values for $P_{\rm I}$ and $P_{\rm II}$ determined for the ferrimagnetic and antiferromagnetic states, respectively, the observed intensities of the intermediate state listed in Table I were substituted into Eqs. (2) to obtain values for Φ_i and Φ_j. For $l=N$ and $l=N\pm\frac{1}{3}$ the values for $\cos\Phi_i$ were -1.03 and -0.735, respectively, and these for $\cos\Phi_j$ were -0.970 or -0.03 and 0.177, respectively.

These solutions did not yield unique values of Φ_i and Φ_j, but suggested values of π or $\pi/2$. The best agreement of relative calculated intensities were obtained for $\Phi_i=\pi$ or $\Phi_j=\pi/2$ as given in Table II. The calculated intensities were too great and any variation in Φ_i or Φ_j to decrease the intensities of $l=N\pm\frac{1}{3}$ reflections causes an increase for those with $l=N$. This indicated that the neutron diffraction intensities were due to a net component of $\cos^2\beta$ times $|F_0|^2q^2$ of Eqs. (2). The net component may be produced by an oscillation angle β of the moments of each layer or by a spiral with a propagation vector τ in the basal plane with a cone angle β.

Calculations of the observed intensity data gave $\cos\beta=0.95\pm0.01$ ($\beta=18°$), $\cos\Phi_i=-1.00\pm0.01$ ($\Phi_i=\pi$), and $\cos\Phi_j=-1.00$ or 0 ± 0.01 ($\Phi_j=\pi$ or $\frac{1}{2}\pi$). The magnetic structure corresponding to the case $\Phi_i=\Phi_j=\pi$ is the single-spin-axis structure of Fig. 3(a) and that for $\Phi_j=\pi/2$ is the two-spin-axis structure of Fig. 3(b). The sequence of phase angles for successive layers of Mn (I) plus adjacent Mn (II) moments is 0, π, π, 0 for single-spin-axis model and 0, $\pi/2$, $-\pi/2$, 0 for the two-spin-axis model.

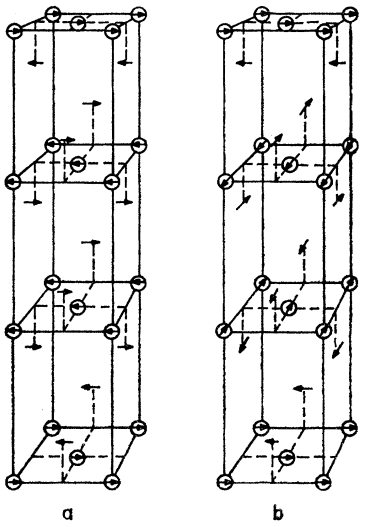

FIG. 3. (a) Single-spin-axis structure and (b) double-spin-axis structure.

A spiral structure with τ in the basal plane should produce additional neutron diffraction satellites lying along a reciprocal lattice row [h00] or [hk0]. According to Koehler's equations,[10] the $\frac{1}{4}\sin^2\beta$ would make the intensities of such satellites very weak, about 2.5% of the triple ferrimagnetic cell reflections. Evidence of such satellites was sought by scans along [100] and [110] reciprocal lattice rows from the strongest ferrimagnetic reflections, (110), (002), and (00 $\frac{5}{3}$). No satellites were detected within the order of 0.5% of the intensities of the ferrimagnetic intensities. This may be due possibly to a nonperiodicity of the propagation vector τ between successive layers.

If the possibility of disorder within a layer is considered, then the angle γ in Eqs. (B1) and (B2) in Appendix B would vary randomly between positive and negative values. Only the terms in cosγ would remain. The net result would be the same as reducing the P_{II} by the factor cosγ. A value of $\gamma=25°$ would bring observed and calculated intensities into agreement.

A random deviation from the antiparallel alignment of Mn (I) and Mn (II) moments within a layer does not seem plausible for the intermediate state because there is no such deviation in the ferrimagnetic and antiferromagnetic states at temperatures just above and below the temperature range over which the intermediate state exists. A magnetic disorder in which the angles between the net moments of the layers deviates randomly from average values seems much more likely because the interlayer exchange energy should be small in the intermediate state. This exchange energy must pass through zero during a ferrimagnetic to antiferromagnetic transition, and the intermediate state of the $x=0.03$ crystal exists only in a narrow temperature range between the ferrimagnetic and antiferromagnetic states.

MAGNETIC-MOMENT CALCULATIONS

The magnetic moments of the two sublattices for the ferrimagnetic and antiferromagnetic states were calculated from neutron-diffraction data. Those for the Mn_2Sb ferrimagnetic state above the anisotropy change were calculated from the (110), (111), and (101) reflections, while those for the lower Mn_2Sb ferrimagnetic state were calculated from the (001), (002), (003), and (110) reflections. The values are given in Table III. For the antiferromagnetic state, the (00l) series of reflections and the (11$\frac{1}{2}$) reflections were used. Table IV lists the calculated moments. The Mn_2Sb form factors agreed with values obtained from simultaneous solutions of the five (00l) antiferromagnetic reflections measured out to $\sin\theta/\lambda$ of 0.42 at room temperature for $Mn_{1.9}Cr_{0.1}Sb$. Figure 4 shows the temperature dependence of the moments in both the ferrimagnetic and antiferromagnetic states. The apparent increase in the moment of Mn (II) and in the net moment per atom at the ferrimagnetic to antiferromagnetic transition in $Mn_{1.9}Cr_{0.1}Sb$ is not consistent with the Hall effect measurements of Bierstedt[12] which show no change in the number of carriers at the transition. Also the net moment per atom in the ferrimagnetic state is lower than that obtained by Darnell *et al.*[4] from saturation

TABLE III. Magnetic moments of the ferrimagnetic state of $Mn_{2-x}Cr_xSb$.

Temperature (°C)	Magnetic moments in μ_B Mn (I)	Mn (II)	Net moment per Mn atom
	For $Mn_{1.9}Cr_{0.1}Sb$		
54	1.69±0.07	2.19±0.08	0.25
75	1.65±0.07	2.06±0.08	0.21
110	1.46±0.07	1.88±0.08	0.21
154	1.22±0.1	1.46±0.10	0.12
200	0.77±0.1	0.94±0.10	0.08
	For $Mn_{1.95}Cr_{0.05}Sb$		
23	1.57±0.07	2.92±0.10	0.67
−16	1.64±0.07	3.06±0.10	0.71
−33	1.63±0.07	3.23±0.10	0.80
	For $Mn_{1.97}Cr_{0.03}Sb$		
−135	1.82±0.07	3.85±0.12	1.01

TABLE IV. Magnetic moments of the antiferromagnetic state of $Mn_{2-x}Cr_xSb$.

Temperature (°C)	Magnetic moments in μ_B Mn (I)	Mn (II)	Net moment per Mn atom
	For $Mn_{1.9}Cr_{0.1}Sb$		
24	1.70±0.07	2.50±0.10	0.40
−15	1.87±0.07	2.67±0.10	0.40
−100	1.88±0.07	3.03±0.10	0.57
−195[a]	1.84±0.10	2.84±0.15	0.50
	For $Mn_{1.95}Cr_{0.05}Sb$		
−99	1.75±0.07	3.58±0.12	0.86
−116	1.83±0.07	3.55±0.12	0.91
	For $Mn_{1.97}Cr_{0.03}Sb$		
−169	1.70±0.07	3.59±0.12	0.95
−196[a]	1.76±0.10	3.68±0.15	0.96

[a] From measurements of crystal in liquid nitrogen.

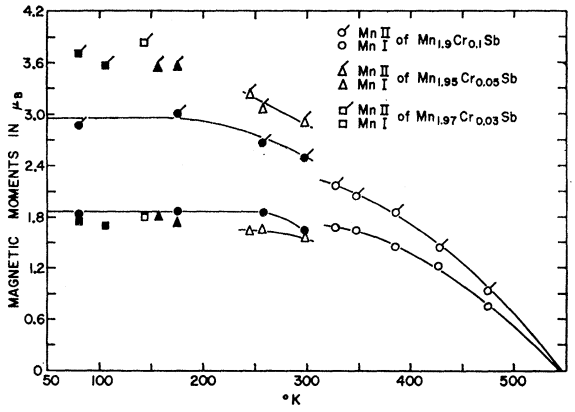

FIG. 4. Plot of magnetic moments versus temperature: open symbols denote ferrimagnetic state; solid symbols denote antiferromagnetic state.

[12] P. E. Bierstedt (to be published).

magnetization measurements. It is suspected that the values of Mn (II) moment for the ferrimagnetic state of $Mn_{1.9}Cr_{0.1}Sb$ given in Table III may be too low, although a source of error in the neutron-diffraction data that might lead to the low values has not been found. The transition in $Mn_{1.95}Cr_{0.05}Sb$ was quite broad, extending from about -50 to -90°C, and involved a partial anisotropy change in the ferrimagnetic state as evidenced by a small increase in the normal $(00l)$ reflections within this temperature range.

In Fig. 5 the temperature dependence of the Mn (I) and Mn (II) moments for the compositions $x=0.05$ and $x=0.1$ is compared with the molecular field solutions discussed in Ref. 4. The neutron-diffraction results show the different temperature dependence of the two sublattices predicted by the molecular-field solutions.

The magnetic moment of Mn (II) decreases with increasing chromium content from that reported for Mn_2Sb, while that of Mn (I) appears to undergo an initial decrease followed by a slight increase over the range of compositions studied. Figure 6 is a plot of the magnetic moments of the antiferromagnetic structure extrapolated to 0°K compared with those of Mn_2Sb.[5,13] Magnetization data[1] have given evidence of a decrease of net moment with addition of chromium. This is confirmed by the present data for the highest chromium content. However, for the lower chromium compositions, the net moment is about the same within the range of error.

The possibility was considered that the antimony atoms possess some magnetic moment. Calculations were made from the data of the $Mn_{1.9}Cr_{0.1}Sb$ crystal in the ferrimagnetic state. An identical form factor was assumed. The solutions of the structure factor equations gave the manganese values essentially unchanged and antimony moments of $0.019\pm0.10\,\mu_B$ at 200°C. These results are in agreement with those of Wilkinson[5] on

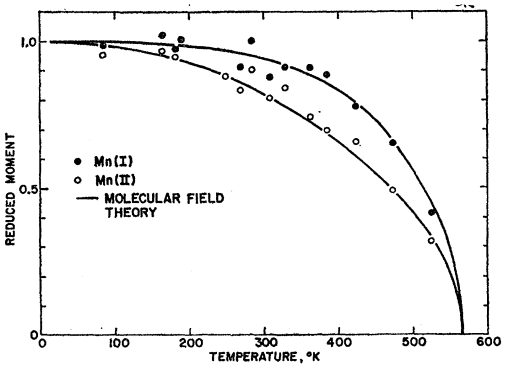

FIG. 5. Reduced sublattice moments of $Mn_{1.95}Cr_{0.05}Sb$ and $Mn_{1.9}Cr_{0.1}Sb$ compared with the results of molecular field theory.

[13] Reference 9 gives values of the atomic moments of Mn_2Sb at room temperature that are lower than those of Ref. 5 but does not give values at low temperature.

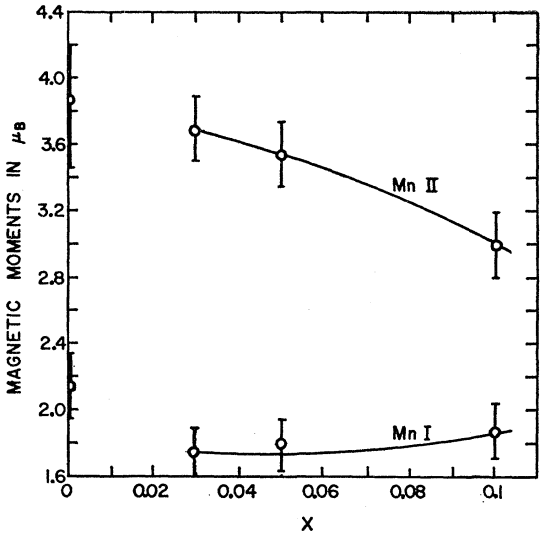

FIG. 6. Variation of magnetic moments with chromium content in $Mn_{2-x}Cr_xSb$ extrapolated to 0°K.

Mn_2Sb and indicate that the antimony atoms do not have a magnetic moment.

CONCLUSIONS

Chromium-modified $Mn_{2-x}Cr_xSb$ can exist in three magnetic states depending upon temperature and chromium content. With decreasing temperature, the order changes from the ferrimagnetic Mn_2Sb structure to a weakly ferrimagnetic structure and than to an antiferromagnetic state. In all of these structures there is antiferromagnetic coupling between layers of Mn (I) atoms and the adjacent Mn (II) atoms.

In the Mn_2Sb ferrimagnetic structure, the magnetic unit cell is identical with the nuclear or chemical unit cell, with ferromagnetic coupling between successive ferrimagnetic layers. In this structure the spins are parallel to the c axis at high temperatures and perpendicular at low temperatures. The antiferromagnetic structure has a unit cell doubled along the c axis, resulting from antiferromagnetic coupling between successive ferrimagnetic layers. For the compositions studied the spins were perpendicular to the c axis, even though the transition may be from either the high- or low-temperature spin orientation of the ferrimagnetic state depending upon the chromium content. The weakly ferrimagnetic state exists for compositions with $x=0.023$ and $x=0.03$. This intermediate structure has a magnetic unit cell with a c axis three times that of the chemical unit cell. It has two possible structures that are indistinguishable by unpolarized neutron diffraction. The angles between moment directions in successive ferrimagnetic layers go in the sequence π, 0, π or $\frac{1}{2}\pi$, π, $\frac{1}{2}\pi$. There appears to be some magnetic disorder in the structure consisting of a small random deviation in the angle between successive layers. The deviation angle was found to be about 18 degrees.

ACKNOWLEDGMENTS

The crystals used were prepared by Dr. J. J. Cox and Dr. K. B. Keating. The authors are indebted to Dr. H. S. Jarrett for many helpful discussions.

APPENDIX A. CHROMIUM DISTRIBUTION

The chromium could possibly substitute for the manganese either at random or preferentially in one of the two manganese equivalent sites. No nuclear superlattice reflections were detected, thus, there is no evidence of ordering of chromium in either the Mn (I) or Mn (II) sites. Therefore, calculations were made for the composition with highest chromium content for comparison with observed nuclear intensities at 24°C. At this temperature the crystal was in the antiferromagnetic state and there were no magnetic contributions to the normal nuclear reflections. The neutron scattering amplitudes in 10^{-12} cm units were -0.37 for manganese, 0.35 for chromium, and 0.54 for antimony. Table V lists observed and calculated relative intensities. The comparison, particularly of the sensitive (202) and (303) reflections, favors chromium substituted at random in the Mn (I) sites.

TABLE V. Comparison of calculated and observed neutron-diffraction reflections for $Mn_{1.9}Cr_{0.1}Sb$ at 24°C.

Reflection	Observed	Calculated for chromium in Random	Mn (I)	Mn (II)
(110)	1.00	1.00	1.00	1.00
(220)	0.084	0.027	0.036	0.020
(330)	0.30	0.29	0.29	0.29
(200)	0.057	0.046	0.060	0.035
(400)	0.018	0.017	0.023	0.013
(101)	1.00	1.00	1.00	1.00
(202)	0.173	0.208	0.142	0.28
(303)	0.241	0.197	0.185	0.19
(001)	0.70	0.75	0.74	0.815
(002)	1.00	1.00	1.00	1.00
(003)	0.186	0.183	0.22	0.16
(004)	0.018	0.015	0.008	0.021
(005)	0.204	0.24	0.27	0.225
(006)	0.41	0.41	0.41	0.32

The magnitude of the magnetic structure factors is dependent upon the nuclear structure factors used in the intensity conversion. Moments were calculated from the magnetic structure factors of (110), (101), and (111) reflections for the ferrimagnetic state at 50°C obtained according to the varying nuclear values for the different chromium distributions. The (101) magnetic component came only from the Mn (II) atoms. The simultaneous solutions of these reflections gave agreement in magnetic moments only for chromium in Mn (I) sites. Table VI lists the magnetic scattering amplitudes given by these solutions for the three choices of chromium substitution. Therefore, it was concluded that the chromium substituted preferentially in the Mn (I) sites.

TABLE VI. Magnetic scattering amplitude variation with chromium distribution in $Mn_{1.9}Cr_{0.1}Sb$ at 50°C.

Chromium distribution	Mn (I) (110) and (101)	Mn (I) (110) and (111)	Mn (II) (110) and (111)	Mn (II) (101)
In Mn (I)	0.44	0.45	0.58	0.59
At random	0.64	0.49	0.69	0.55
In Mn (II)	0.81	0.56	0.79	0.54

APPENDIX B

Calculated Intensities for Deviations in Phase Angle

The deviation of phase angles from π between adjacent Mn (I) and Mn (II) spins in the basal plane can be expressed as $\pi \pm \gamma$. For a periodic lattice within one domain the sign of γ must be assigned with the z parameter of the triple cell. This leads to sine terms in the complex structure factor, F, and the equations for $|F|^2$ $(00l)$ of the triple unit cell are as follows:

For the single-spin-axis system:

$$|F|^2(00l) = [4(P_{\mathrm{I}} - P_{\mathrm{II}} \cos 2\pi lz \cos\gamma)^2 + |2P_{\mathrm{II}} \sin 2\pi lz \sin\gamma|^2] \times [1 - 2\cos(2\pi l/3)]^2 \quad \text{(B1)}$$

and for the system of two perpendicular spin axes:

$$|F|^2(00l) = [2(P_{\mathrm{I}} - P_{\mathrm{II}} \cos 2\pi lz \cos\gamma) - 4P_{\mathrm{II}} \sin(2\pi l/3) \sin 2\pi lz \sin\gamma]^2 + [4\sin(2\pi l/3)(P_{\mathrm{I}} - P_{\mathrm{II}} \cos 2\pi lz \cos\gamma) - 2P_{\mathrm{II}} \sin 2\pi lz \sin\gamma]^2. \quad \text{(B2)}$$

In averaging over all domains this equation reduces to

$$|F|^2(00l) = [1 + 4\sin^2(2\pi l/3)] \times [4(P_{\mathrm{I}} - P_{\mathrm{II}} \cos 2\pi lz \cos\gamma)^2 + (2P_{\mathrm{II}} \sin 2\pi lz \sin\gamma)^2], \quad \text{(B3)}$$

where l and z are the index and parameter of the triple cell. Calculations according to these equations indicate increased intensity for nonobserved satellite reflections such as (002) and (008). A deviation angle γ of 25 deg would be required to bring the $|F|^2$ values of the strong satellites (004) and (005) into agreement with observed ones. For this angle the calculated value of the normal ferrimagnetic reflection (003) is increased and those of (002) and (008) are equal to or greater than that of the (003). If the deviation angle γ were in a vertical plane, then the sine terms for the $(00l)$ reflections would vanish, leaving just the cosine terms which would decrease the calculated values to approximate agreement. However, then there would be a corresponding increase in the calculated values for the (hhl) reflections which leads to greater disagreement with the observed data.